Picosecond time-resolved imaging using SPAD array cameras

Genevieve Gariepy[a], Jonathan Leach[a], Ryan Warburton[a], Susan Chan[a], Robert Henderson[b], and Daniele Faccio[a]

[a]Institute of Photonics and Quantum Sciences, Heriot-Watt University, EH14 4AS Edinburgh, UK.

[b]Institute for Micro and Nano Systems, University of Edinburgh, Alexander Crum Brown Road, Edinburgh EH9 3FF, UK.

ABSTRACT

The recent development of 2D arrays of single-photon avalanche diodes (SPAD) has driven the development of applications based on the ability to capture light in motion. Such arrays are composed typically of 32x32 SPAD detectors, each having the ability to detect single photons and measure their time of arrival with a resolution of about 100 ps. Thanks to the single-photon sensitivity and the high temporal resolution of these detectors, it is now possible to image light as it is travelling on a centimetre scale. This opens the door for the direct observation and study of dynamics evolving over picoseconds and nanoseconds timescales such as laser propagation in air, laser-induced plasma and laser propagation in optical fibres. Another interesting application enabled by the ability to image light in motion is the detection of objects hidden from view, based on the recording of scattered waves originating from objects hidden by an obstacle. Similarly to LIDAR systems, the temporal information acquired at every pixel of a SPAD array, combined with the spatial information it provides, allows to pinpoint the position of an object located outside the line-of-sight of the detector. A non-line-of-sight tracking can be a valuable asset in many scenarios, including for search and rescue mission and safer autonomous driving.

Keywords: temporal imaging, single photon detection

Capturing light in motion presents an interesting challenge, as a resolution of the order of 100 picosecond is needed to freeze flight on a centimetre scale. The ability to do so opens the door to diverse applications, both for fundamental studies of optical phenomena and for sensing applications such as 3D imaging and non-line-of-sight object detection. Much effort has therefore been made in the last decades to develop methods that allow to visualise light in motion, or perform "light in flight" measurements. This term was coined in 1978 by Abramson,[1] who developed a technique based on holography to record the dynamics of light phenomena such as reflection, focusing and interference. To record the propagation of light, short pulses were sent onto a scattering surface at a grazing angle in such a way that the laser beam intercepted the surface at different times at different points and then scattered light towards a holographic plate. The holographic plate was simultaneously illuminated by a reference beam, also composed by short pulses of light incident at an angle. The hologram hence captured the spatial distribution of the scene at different times, and illuminating the recorded hologram plate at different positions allowed to play back a movie of light propagating across the scattering surface, with a resolution of about 10 ps. Since this seminal work, different techniques have been developed to push the limits of light-in-flight imaging. Velten *et al*. have shown that streak cameras can be used to perform measurements of laser pulses propagating in a scattering medium or across a scene with high temporal and spatial resolution,[2] and Gao *et al*. have demonstrated a single-shot implementation of such a technique.[3] Photonic mixer devices can also be used to perform transient imaging, i.e. to record diffuse light as it illuminates a scene, for a much lower budget and form factor than with using streak cameras, although at the cost of lower temporal resolution (∼10 ns).[4] Although impressive visualisations of light-in-motion have been achieved with these techniques, they all relied on the use of a scattering medium or surface to enhance the signal sent to the detector. We report here on a novel method to capture light in motion with 100 ps resolution that is both compact and easy-to-use, and allows

Further author information: (Send correspondence to D. Faccio)
E-mail: d.faccio@hw.ac.uk

Emerging Imaging and Sensing Technologies, edited by Keith L. Lewis, Richard C. Hollins, Proc. of SPIE Vol. 9992, 99920N · © 2016 SPIE
CCC code: 0277-786X/16/$18 · doi: 10.1117/12.2241184

the direct recording of events of very low intensity level such as laser pulse propagation in air.[6] We then discuss applications of this technology. We also note that although this is largely a review, much of the material is actually including the data Figs. 2, 4, 5 and relative discussion in the text.

Our method is based on the use of a 32x32 single-photon avalanche diode (SPAD) array, where each pixel is formed by an active element capable of detecting single photons, and time-correlated-single-photon-counting (TCSPC) electronics that measure the photons arrival time with a resolution of ~ 50 ps (time bin width) and with an impulse response function time of 110 ps.[5] This detector can therefore be used to collect three-dimensional information (x, y, t) about a scene by collecting individual photons for each frame and building up histograms of their arrival time on each pixel of the array.

In an experiment illustrated in figure 1, we observe the propagation of laser pulses as they travel through air. Short pulses from a femtosecond oscillator (800 nm, 10 nJ, 10 fs) are emitted at 67 MHz and directed in front of the SPAD camera. A series of mirrors deflect their path so that the laser beam crosses the field of view 3 times. On their path, the pulses undergo scattering interactions with air molecules, so that some light is scattered from the path onto the detector. Given the single-photon sensitivity of the SPAD camera, we are able to record the laser propagation by detecting only these scattered photons, with no need for an additional scattering medium to enhance the signal reaching the detector. A similar experiment done with a 4 kHz microchip laser at 532 nm is reported in.[6]

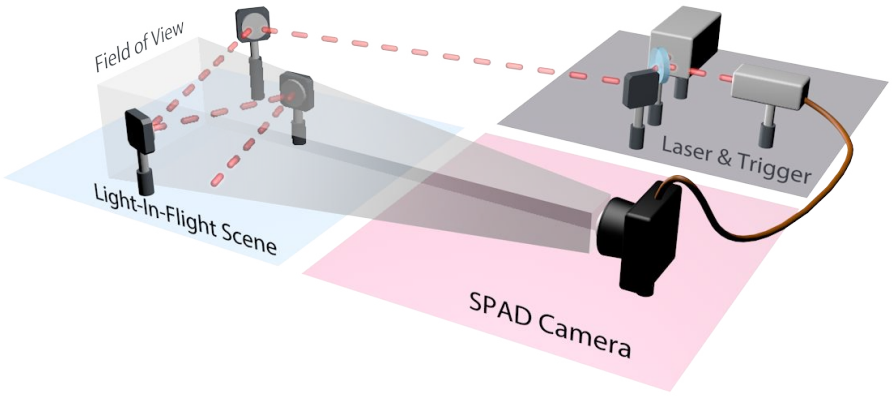

Figure 1. To capture the propagation of laser pulses in air, we direct femtosecond pulses across the field of view of the SPAD camera. Photons scattered by air molecule in the laser's path are detected by the 32x32 pixels of the SPAD array, and their time of arrival is measured with respect to a trigger synchronised with the emission of the pulses. An acquisition results in a three-dimensional data sets containing spatial and temporal (x, y, t) information, showing the time evolution of the pulses with a temporal resolution of 110 ps.

In figure 2, we show an example of the data recorded with the SPAD camera. The data was processed by first subtracting a background acquired without the pulse propagating across the field of view, to suppress the noise in the data, and by identifying peaks in the histograms and fitting a Gaussian to the peaks above a given threshold. The data can then be visualised as a video of the laser pulses propagating across the field of view,

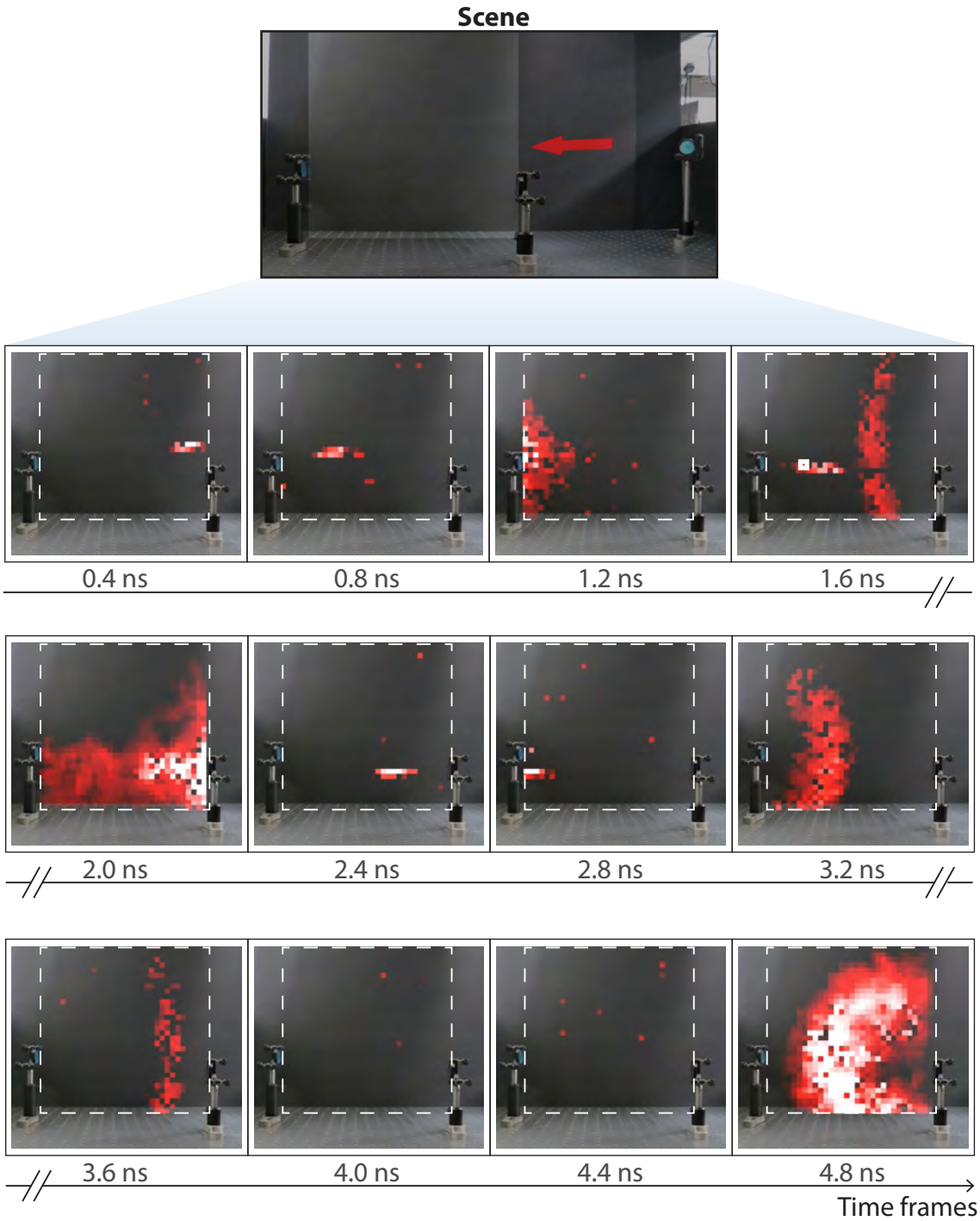

Figure 2. A light-in-flight measurement performed with the SPAD camera allows to observe the evolution of laser pulses as they propagate through air. In addition to the pulse itself, we also measure signals originating from the scattered part of the light at each reflection on the mirrors. This scattered wave, generated at each reflection, creates a flare effect on the camera (frames 1.2 ns and 2.0 ns), but also propagates in all directions. In particular, part of this wave reaches a black cardboard placed at the back on the scene and the spherical wavefront of the wave sweeping across the cardboard is recorded by the camera (frames 1.6 ns, 3.2 ns, 3.6 ns and 4.8 ns

by playing back the given spatial frames (x, y) corresponding to different measured times t. In figure 2, the SPAD data has been overlaid onto a picture of the scene taken with a standard DSLR camera, which shows the experimental setup. The short laser pulse can be observed as it enters the field of view and propagates to the left (frame 0.4 ns and 0.8 ns), is reflected towards the right (frame 1.6 ns) and is reflected once more before exiting the field of view (2.4 ns and 2.8 ns).

We also observe in figure 2 another interesting signal. At every reflection on a mirror, most of the beam is reflected, but there is a portion that is scattered, approximately as a spherical wave, and propagates in all directions. This scattered wave creates a flare effect that can be observed in frame 1.2 ns as the laser is reflected on the left mirror and in frame 2.0 ns as the laser is reflected on the last mirror on the right of the field of view. This flare, i.e. scattering is created by a thin film of dust or dirt that apparently accumulates on the mirror surface, and is present even if to the eye the surface looks perfectly clean. At later times, we capture another part of that scattered (spherical) wave as it reaches the black cardboard placed at the back of the scene. The spherical wave intersects this cardboard in a way that a section of the spherical wavefront is recorded by the camera as it travels across the field of view. In frame 1.6 ns, we can observe a wave originating from the first mirror on the right, as it sweeps across the back of the scene towards the left. Later, in frames 3.2 ns and 3.6 ns, the wave originating from the left mirror is observed propagating to the right, and finally we detect the same type of signal from the last mirror in frame 4.8 ns. This type of spherical wave signal is of particular interest as it contains information about objects located outside the field of view of the camera. Indeed, we can observe in figure 2 that the shape of the recorded wavefronts points to the position of the mirrors that are located outside the field of view and from where the scattered waves originate.

We exploited this type of detected signal and information to develop a method that allows to detect objects not only outside the field of view of the camera, but physically hidden from view by an obstacle. The detection principle is illustrated in figure 3. Here, an object is hidden from the camera by a wall. To send a signal around this obstacle, we use short pulses of light (780 nm, ∼500 mW average power, 80 MHz) and direct them on a surface in our line-of-sight, but beyond the edge of the obstacle. For example, here the laser pulses are directed onto the floor and the SPAD camera images a section of the floor that is also beyond the edge of the wall. As illustrated in figure 3b, when the laser hits the floor, light is scattered in all directions and travels into the hidden scene. An object hidden in this scene will scatter back a signal which will cross the field of view. Similarly to the signals shown in figure 2, the shape of the detected wavefront will contain information about the position of the object, including also its time of arrival which in turn contains additional information about the object distance. The algorithm used to retrieve the objects position, as well as a proof-of-principle experiment at small scale (30 cm high object located 1 m away from the camera), have been reported in.[7] To retrieve the position of a hidden object we first measure the time of arrival of the signal of interest of each of the 32x32 pixels of the SPAD array. For a pixel imaging a spot on the floor at position $\vec{r}_i$, the time of flight measured at this pixel corresponds to the time of flight of the laser pulses between the laser spot on the floor $(\vec{r}_l)$ and the object $(\vec{r}_o)$, and between the object and the pixel i. An object could be situated anywhere along an ellipse described by $|\vec{r}_o - \vec{r}_l|^2 + |\vec{r}_i - \vec{r}_o|^2 = c\langle t\rangle_i$ to produce a signal at position $\vec{r}_i$ detected at time $\langle t\rangle_i$. For each pixel of the array, we therefore calculate this elliptical probability of finding the object at a position $\vec{r}_o$; multiplying the probability densities found for each pixel leads to a joint probability density that points to the object location. The results from the first experiment demonstrated that this technique can be used to locate objects with centimetre precision with 3 seconds acquisition time for an object located about a metre away from the camera, thus making it possible to track the motion of an object moving at a few centimetres per second in real-time.[6]

We report here on experiments performed at larger scales to study the possibility of using this technique to detect people hidden from view a few metres away from the detector, which is a scale more relevant to applications in real-life scenarios. We positioned the camera 1 metre above the floor, looking down at a 20x54 cm area on the floor 2.1 metres away. The laser pulses were sent onto the floor, below the field of view to avoid a strong

reflection to saturate the detection. A person was then positioned at different points on the left, hidden from the camera by an obstacle. The geometry of this experiment is shown, to scale, in figure 3.

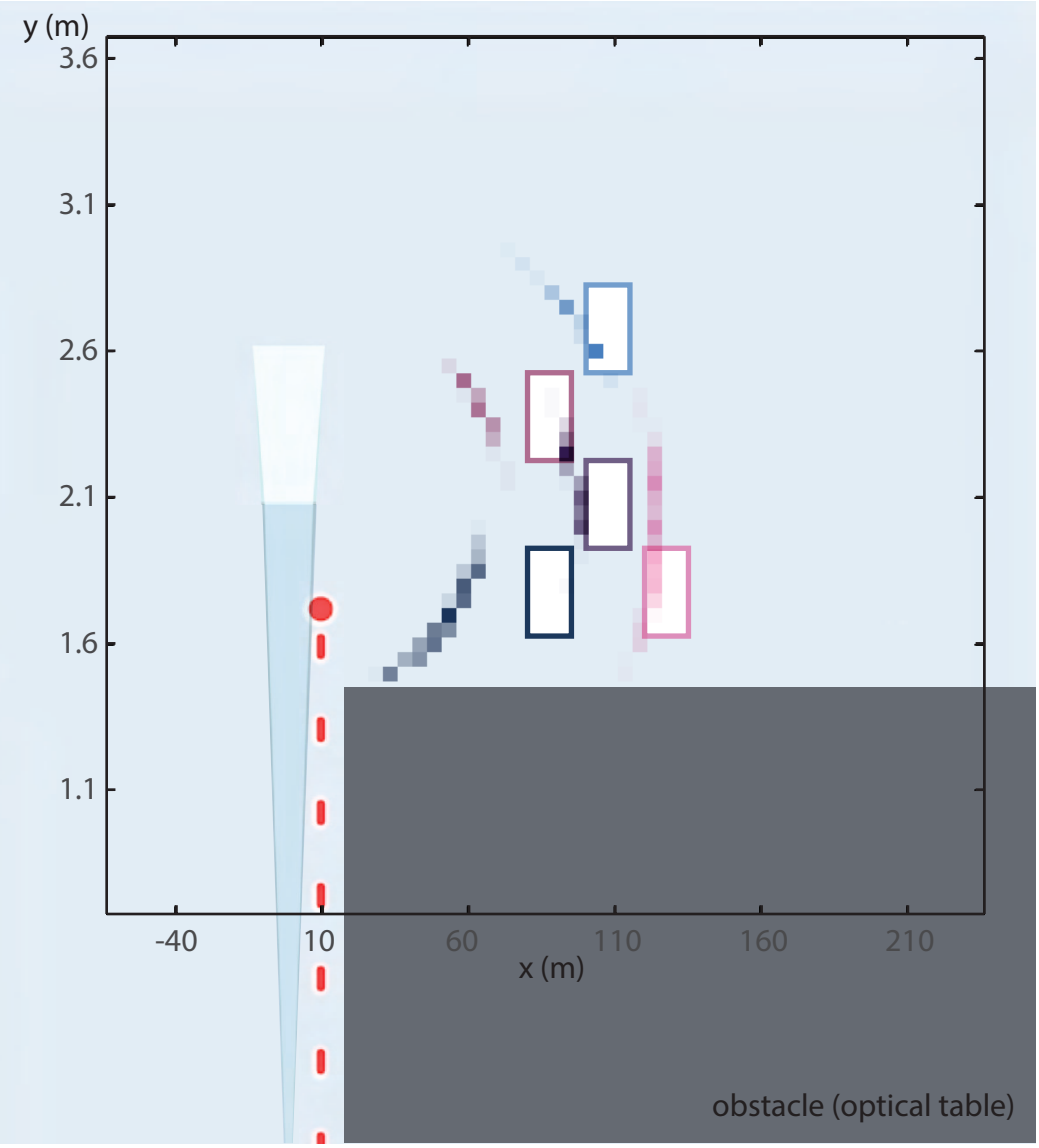

Figure 3. A measurement was performed with the SPAD camera looking down at the floor 2.1 metres away. A 30-second acquisition time allowed us to record enough signal to isolate a signal from a person hidden from view around an obstacle. We find the time of arrival of this signal on every pixel of the SPAD camera and use it to retrieve a probability density of the object position around the obstacle. The probability densities are shown here and the actual position of the hidden person is indicated by a rectangle of the corresponding contour colour.

We found that, in this geometry where the hidden object is farther away, a 3 second acquisition was not sufficient to acquire enough signal to detect the hidden target. We therefore integrated the signal over 30 seconds. The signal from the target is isolated in a similar way than that reported in,[7] where a background is subtracted to the acquired data to isolate the signal of interest from all other signals coming from the environment. A Gaussian is fitted to each detected histogram to find the signal arrival time at each pixel, and this information is used to retrieve the hidden object's position. In figure 3, we show the retrieved probability densities for the

object position in the hidden area, calculated using our algorithm based on elliptical probability densities for each pixel, and for five different positions of the target. The resulting probability densities are in good agreement with the actual positions. However, in this implementation of our method, we are limited to detecting targets up to about 1 metre away from the field of view in an acquisition time that is too long to perform real-time tracking. As we will discuss below, expected improvements to the hardware will allow us to reduce the acquisition times and increase the target's distance.

We also investigated a geometry where the camera is looking towards a wall in its line-of-sight, rather than the floor, to detect a signal from a hidden target. Since the scattering from the diffuse surfaces in the experiment is not isotropic but is preferential in a direction normal to the surface, we found that more signal can be detected using a wall than the floor. In figure 4, we show the signal acquired with the SPAD camera located 5 metres away from the wall, for three different positions of a hidden person. We observe that the signal recorded is dependent on the distance between the person and the field of view, but also on its exact position. We find that a similar signal is recorded in a 30 seconds acquisition time for a person hiding at position 1, 1.5 metres away from the field of view along the wall; at position 2, 3 metres away in front of the wall and at position 3, at an intermediary position 2.5 metres away from the field of view. Although this signal was acquired in with a long acquisition time, the recorded signals shown in figure 4b illustrate that it is possible to detect a person hiding up to 8 metres from the camera.

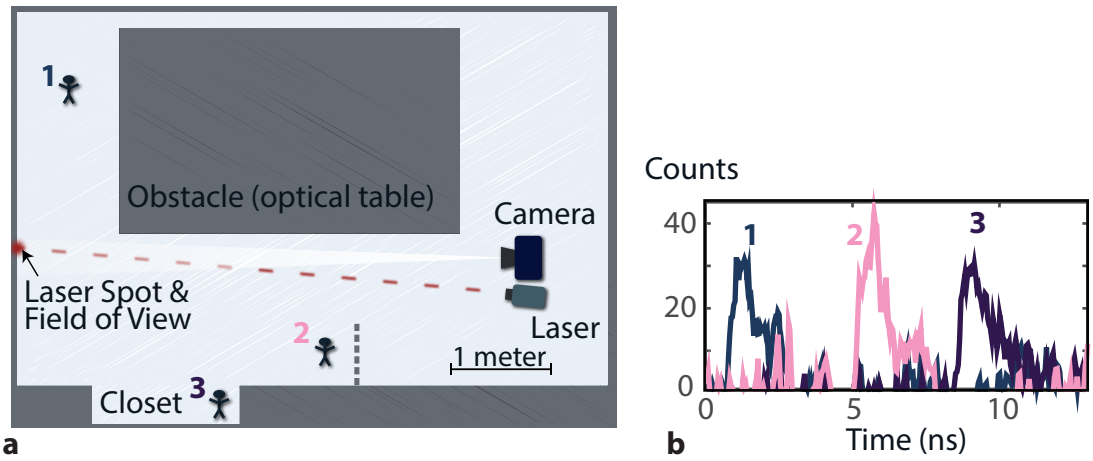

Figure 4. a) We detect a signal over a 30 seconds acquisition time for a person hiding at three positions in the laboratory. At position 1, the person is placed 1.5 m away from the field of view, along the wall. It is hidden from the camera by an optical table. At position 2, the person is not physically hidden from the camera, but is outside its line-of-sight and could technically be hidden by a wall indicated by the dashed line. At position 3, the person is physically hiding in a closet with the door open. The amount of light received by the hidden person at these different positions is different due to the lambertian scattering profile of the laser pulses on from the wall. b) We observe in the histograms recorded at a given pixel of the camera that the signal recorded is equivalent at those three positions. This signal can be used to retrieve the position of the hidden person.

Improvements to the performance of our non-line-of-sight detection system at human scales are expected by advances in the detection hardware. In particular, the overall efficiency of the camera is limited by the low efficiency of the SPAD detectors at our operating wavelength (6.5% at 780 nm) and its low fill factor (2%). Advances in the design of SPAD arrays promise to increase the fill factor by a factor up to 40x and using a detector optimised for our operating wavelength could allow us to reach detection efficiency of 20-30%, increasing the overall efficiency by another factor 5x. The read-out rate of the SPAD array is also currently limited by its USB2.0 connection at 3 kHz, and next generations of SPAD arrays should incorporate a USB3.0 connection to increase the read-out rate and hence the total signal that can be acquired within a few seconds acquisition time,[8] by a factor ∼10x.

When considering the scaling up of such a system, two distances are important to consider: the distance between the target and the area of the scattering surface image $\approx \vec{r}_o$, and the distance between the camera and the scattering surface (floor or wall) r_w. In the first case, an object placed farther away from the field of view will lead to a decrease in signal in $\sim 1/|\vec{r}_o|^4$, as light undergoes two scattering events and looses intensity in $1/r^2$ as it travels between those points as a spherical wave. In the case of the stand-off distance between the camera and the wall, it is possible to compensate for the loss of signal due to the fact we are imaging a scattered signal (giving a loss that scales as $1/r_w^2$ between the wall and the camera) by optimising the collection optics. Indeed, the collected signal depends not only on the distance r_w, but also on the diameter of the collection optics, d_c, and the size of the field of view on the wall corresponding to the detection area, d_w. If we consider for example, the collection onto a detector using a fibre component of given core diameter and numerical aperture NA $= \sin\theta$, the optimal signal collection is achieved when the imaging optic used to collect light matches the NA of the fibre. Assuming an imaging system that respects the single lens equation, we find that there is an optimum collection optics diameter d_c for an imaging optic of a given focal length that increases with focal length. On the other hand, an increase with focal length decreases the spot size on the wall d_w. For a given focal length and collection optic matching the NA of the collection fibre, we find that the product of these two dimensions is

$$d_c \times d_w \propto 2 r_w \tan\theta \tag{1}$$

The collected signal is proportional to both areas ($\propto d_c^2 \times d_w^2$), so we find that we can compensate perfectly the loss in $1/r_w^2$ as the camera gets farther away by using optimal collection optics that will lead to a bigger collection diameter and imaging spot that scales as r_w^2. As an example, the optimal characteristics for a collection into a fibre core of 62.5 μm with NA = 0.22 are shown in figure 5 for a distance r_w = 50 m and 500 m.

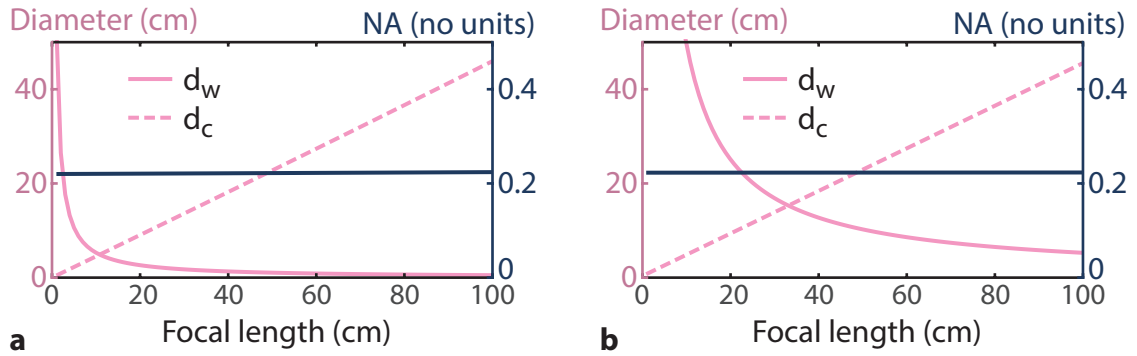

Figure 5. To optimise the signal detection onto a detector of given area and numerical aperture, we use an imaging system whose numerical aperture matches that of the detector. We calculate the optimal diameter of the collection optics at various focal length for collection into an optical fibre of 62.5!μm core and NA = 0.22 for a wall to camera distance of a) 50 metres and b) 500 metres.

We also find that, for larger distances r_w, a longer focal length is preferable as it leads to a smaller spot size on the wall – it is important to keep the size of this spot lower than the corresponding dimension of the temporal resolution of our system, so as to not blur the information collected. For example, to keep a spot size of 10 cm detected by a single pixel detector, one needs a 20 cm diameter system with a 50 cm focal length for a wall distance of 500 metres, and a 45 cm diameter system with a 1 m focal length for a wall distance of 1 km. Designing a non-line-of-sight tracking with imaging optics close to those optimal values would therefore allow to greatly increase the stand off distance at which measurements can be performed, to a few tens and potentially hundreds of metres.

REFERENCES

[1] Abramson, N., "Light-in-flight recording by holography," *Opt. Lett.* **3**(4), 121–123 (1978).

[2] Velten, A., Wu, D., Jarabo, A., Masia, B., Barsi, C., Joshi, C., Lawson, E., Bawendi, M., Gutierrez, D., and Raskar, R., "Femto-photography: Capturing and visualizing the propagation of light," *ACM Trans. Graph.* **32**(4), 44:1–44:8 (2013).

[3] Gao, L., Liang, J., Li, C., and Wang, L. V., "Single-shot compressed ultrafast photography at one hundred billion frames per second," *Nature* **516**(7529), 74–77 (2014).

[4] Heide, F., Hullin, M. B., Gregson, J., and Heidrich, W., "Low-budget transient imaging using photonic mixer devices," *ACM Trans. Graph.* **32**(4), 45:1–45:10 (2013).

[5] Richardson, J., Grant, L., and Henderson R., "Low dark count single-photon avalanche diode structure compatible with standard nanometer scale cmos technology," *Photon. Technol. Lett.* **21**, 1020-1022 (2009).

[6] Gariepy, G., Krstajic, N., Henderson, R., Li, C., Thomson, R. R., Buller, G. S., Heshmat, B., Raskar, R., Leach, J., and Faccio, D., "Single-photon sensitive light-in-flight imaging," *Nat. Commun.* **6**, 6021 (2015).

[7] Gariepy, G., Tonolini, F., Henderson, R., Leach, J., and Faccio, D., "Detection and tracking of moving objects hidden from view," *Nat. Phys.* **10**, 23 (2016).

[8] Krstajić, N., Poland, S., Tyndall, D., Walker, R., Coelho, S., Li, D. D.-U., Richardson, J., Ameer-Beg, S., and Henderson, R., "Improving tcspc data acquisition from cmos spad arrays," in [*Advanced Microscopy Techniques III*], *Advanced Microscopy Techniques III* , 879709, Optical Society of America (2013).